Pure Appl. Chem., Vol. 80, No. 11, pp. 2241–2258, 2008.
doi:10.1351/pac200880112241

Progress on the electrolytes for dye-sensitized solar cells*

Jihuai Wu‡, Zhang Lan, Sanchun Hao, Pingjiang Li, Jianming Lin, Miaoliang Huang, Leqing Fang, and Yunfang Huang

The Key Laboratory of Functional Materials for Fujian Higher Education, Institute of Materials Physical Chemistry, Huaqiao University, Quanzhou 362021, China

Abstract: Dye-sensitized solar cells (DSSCs) have aroused intense interest over the past decade owing to their low cost and simple preparation procedures. Much effort has been devoted to the study of electrolytes that enable light-to-electrical power conversion for DSSC applications. This review focuses on recent progress in the field of liquid, solid-state, and quasi-solid-state electrolytes for DSSCs. It is believed that quasi-solid-state electrolytes, especially those utilizing thermosetting gels, are particularly applicable for fabricating high photoelectric performance and long-term stability of DSSCs in practical applications.

Keywords: dye-sensitized solar cells; liquid electrolytes; solid-state electrolytes; quasi-solid-state electrolytes; photoelectric performance; long-term stability.

INTRODUCTION

The development of new types of solar cells is promoted by increasing public awareness that the earth's oil reserves could run out during this century. As the energy need of the planet is likely to double within the next 50 years and frightening climatic consequences of the greenhouse effect caused by fossil fuel combustion are anticipated, it is urgent that we develop a new kind of renewable energy to cover the substantial deficit left by fossil fuels. Among the sources of renewable energy, solar energy is considered the most promising. Fortunately, the supply of energy from the sun to the earth is gigantic: 3×10^{24} J a year, or about 10 000 times more than the global population currently consumes. In other words, covering 0.1 % of the earth's surface with solar cells with an efficiency of 10 % would satisfy our present needs. But tapping into this huge energy reservoir remains an enormous challenge [1].

Since the prototype of a dye-sensitized solar cell (DSSC) was reported in 1991 by M. Grätzel [2], it has aroused intense interest owing to its low cost, simple preparation procedure, and benign effect on the environment compared with traditional photovoltaic devices [1–4]. In "Grätzel cells", the functions of light absorption and charge-carrier transportation are separated, which is different from photoregenerative and -synthetic cells [1]. Although the solar power conversion efficiencies of DSSCs are lower than that of classical crystalline silicon cells, there is a high potential for improvement in efficiency, since it still is far from the theoretical efficiency [5].

In DSSCs based on liquid electrolytes, a photoelectric conversion efficiency of 11 % has been achieved [3,4]. However, the potential problems caused by liquid electrolytes, such as the leakage and volatilization of solvents, possible desorption and photodegradation of the attached dyes, and the cor-

*Paper based on a presentation at the 3rd International Symposium on Novel Materials and Their Synthesis (NMS-III) and the 17th International Symposium on Fine Chemistry and Functional Polymers (FCFP-XVII), 17–21 October 2007, Shanghai, China. Other presentations are published in this issue, pp. 2231–2563.

‡Corresponding author: Tel.: +86 595 22693899; Fax: +86 595 22693999; E-mail: jhwu@hqu.edu.cn

rosion of Pt counterelectrode, are considered as some of the critical factors limiting the long-term performance and practical use of DSSCs [4,6–8]. Therefore, much attention has been given to improving the liquid electrolytes or replacing the liquid electrolytes by solid-state or quasi-solid-state electrolytes [5–10]. This review will focus on progress in the development of improved electrolytes, especially quasi-solid-state electrolytes for DSSCs.

STRUCTURE AND OPERATIONAL PRINCIPLES OF DYE-SENSITIZED SOLAR CELLS

As shown in Fig. 1 [1,3,4], DSSCs include a substrate of fluorine-doped SnO_2 conducting glass (FTO), a porous nanocrystalline semiconductor oxide (the most employed is TiO_2) film sensitized by a dye (typically bipyridine ruthenium complexes) for absorbing visible light, a redox electrolyte (usually an organic solvent containing a redox system, such as iodide/triiodide couple) layer for deoxidizing oxidized dye, and a platinized cathode to collect electrons and catalyze the redox couple regeneration reaction [2]. The light-to-electricity conversion in a DSSC is based on the injection of electron from the photoexcited state of the sensitized dye into the conduction band of TiO_2. The dye is regenerated by electron donation from iodide in the electrolyte. The iodide is restored, in turn, by the reduction of triiodide at the cathode, with the circuit being completed via electron migration through the external load. The voltage generated under illumination corresponds to the difference between the Fermi level of the electron in the TiO_2 and the redox potential of the electrolyte. Overall, the device generates electric power from light without suffering any permanent chemical transformation [1,2,11,12].

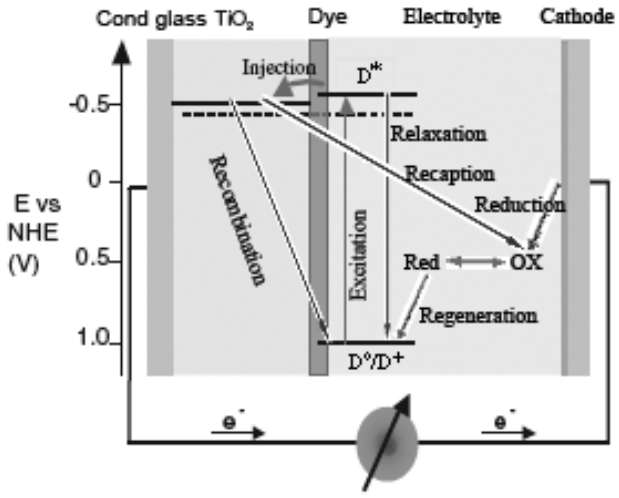

Fig. 1 Principle of operation of DSSCs.

The photoelectric chemical process in DSSC can be expressed as eqs. 1–6. The photoexcited electron injects into the conduction band of TiO_2 in subpicosecond time scales [13–15]. The dark reaction eqs. 5 and 6 also occur during the light-to-electricity conversion, but do not play a remarkable negative effect on photovoltaic performance of DSSCs owing to their slow reaction speed compared with that of eq. 2 [16–18].

$$TiO_2|S + h\nu \rightarrow TiO_2|S^* \quad \text{excitation} \tag{1}$$

$$TiO_2|S^* \rightarrow TiO_2|S^+ + e^-_{(cb)} \quad \text{injection} \tag{2}$$

$$TiO_2|2S^+ + 3I^- \rightarrow TiO_2|2S + I_3^- \quad \text{regeneration} \tag{3}$$

$I_3^- + 2e^-_{(Pt)} \rightarrow 3I^-$ reduction (4)

$I_3^- + 2e^-_{(cb)} \rightarrow 3I^-$ recaption (dark reaction) (5)

$TiO_2|S^+ + e^-_{(cb)} \rightarrow TiO_2|S$ recombination (dark reaction) (6)

It can be seen that DSSCs are a kind of complex system for light-to-electricity conversion. As a basic component, the electrolyte plays an important role in the process of light-to-electricity conversion in DSSCs. The electrolytes employed in DSSCs can be classified as liquid, solid-state, or quasi-solid-state. Several aspects are essential for any electrolytes in a DSSC [5,10].

(1) The electrode must be able to transport the charge carrier between photoanode and counter-electrode. After the dye injects electrons into the conduction band of TiO_2, the oxidized dye must be reduced to its ground state rapidly. Thus, the choice of the electrolyte should take into account the dye redox potential and regeneration of itself.
(2) The electrode must be able to permit the fast diffusion of charge carriers (higher conductivity) and produce good interfacial contact with the porous nanocrystalline layer and the counterelectrode. For liquid electrolytes, it is necessary to prevent the loss of the liquid electrolyte by leakage and/or evaporation of solvent.
(3) The electrolyte must have long-term stability, including chemical, thermal, optical, electrochemical, and interfacial stability, which does not cause the desorption and degradation of the dye from the oxide surface.
(4) The electrolyte should not exhibit a significant absorption in the range of visible light. For the electrolyte containing I^-/I_3^- redox couple, since I_3^- shows color and reduces the visible light absorption by the dye, and I_3^- ions can react with the injected electrons and increase the dark current. Thus, the concentration of I^-/I_3^- must be optimized.

LIQUID ELECTROLYTES

The first DSSC was reported in 1991 by M. Grätzel [2] using organic liquid electrolyte containing LiI/I_2, which obtained an overall light-to-electricity conversion efficiency of about 7.1 % under irradiation of AM 1.5, 100 $mW \cdot cm^{-2}$. Later, many kinds of liquid electrolytes containing iodide/triiodide redox couple and high dielectric constant organic solvents such as acetonitrile (AcN), ethylene carbonate (EC), 3-methoxypropionitrile (MePN), propylenecarbonate (PC), γ-butyrolactone (GBL), and *N*-methylpyrrolidone (NMP) were investigated, and some DSSCs with high photovoltaic performance were obtained [6,19–22]. Research during the past decade shows that each component of liquid electrolyte such as solvent, redox couple, and additive plays a different role in the photovoltaic performance of DSSCs.

Organic solvents

The organic solvent is a basic component in liquid electrolytes, it gives an environment for iodide/triiodide ions' dissolution and diffusion. The physical characteristics of organic solvent including donor number, dielectric constants, viscosity, etc. affect the photovoltaic performance of DSSCs. Especially, the donor number of solvent shows obvious influence on the open-circuit voltage (V_{oc}) and short-circuit current density (J_{sc}) of DSSCs. The donor–acceptor reaction between nonaqueous solvents and iodide to generate triiodide in DSSCs was investigated, the results showed [19] that the extent of transformation from iodide to triiodide ions in a given solvent could be predicted according to the donor number of the solvent. Therefore, the V_{oc} increased and J_{sc} decreased with the increase of the donor number of solvent in liquid electrolytes in DSSCs [20] as shown in Fig. 2. The similar influence of the

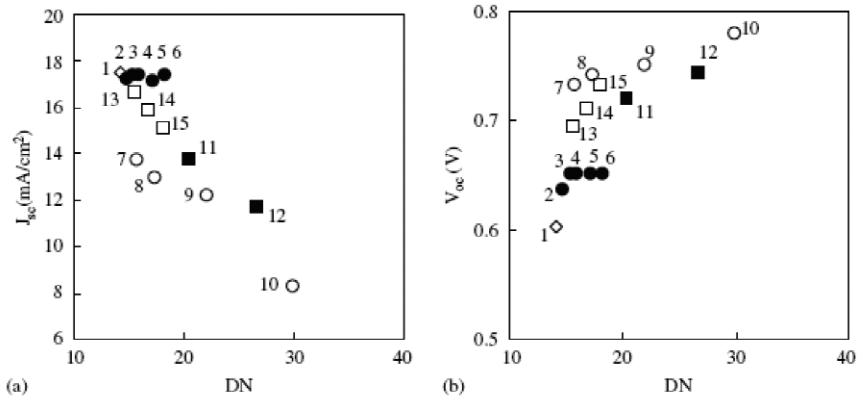

Fig. 2 Dependence of (a) J_{sc} and (b) V_{oc} of DSSCs on the donor number of solvents. (1: AcN, 2: 10 % THF/90 % AcN, 3: 20 % THF/80 % AcN, 4: 30 % THF/70 % AcN, 5: 50 % THF/50 % AcN, 6: 70 % THF/30 % AcN, 7: 10 % DMSO/90 % AcN, 8: 20 % DMSO/80 % AcN, 9: 50 % DMSO/50 % AcN, 10: DMSO, 11: 50 % DMF/50 % AcN, 12: DMF, 13: 10 % NMP/90 % AcN, 14: 20 % NMP/80 % AcN, 15: 30 % NMP/70 % AcN). Electrolyte contains 0.6 M DMPII, 0.1 M LiI, 0.05 M I_2.

donor number of solvents in liquid electrolytes on the photoelectric performance of DSSCs also was found by another group [23].

Our research group [22] investigated the influence of the donor number of the mixed solvent with GBL and NMP on the photoelectric performance of DSSCs. The same results as the above were obtained and shown in Fig. 3.

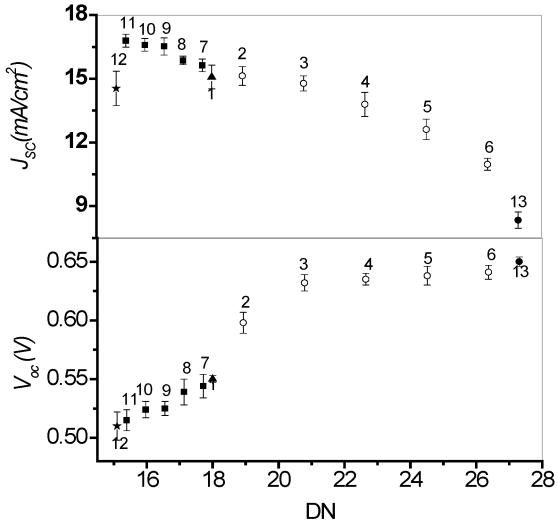

Fig. 3 V_{oc} and J_{sc} of DSSCs as functions of the donor number of solvents. (1: GBL; 2: 10 % NMP/90 % GBL; 3: 30 % NMP/70 % GBL; 4: 50 % NMP/50 % GBL; 5: 70 % NMP/30 % GBL; 6: 90 % NMP/10 % GBL; 7: 10 % PC/90 % GBL; 8: 30 % PC/70 % GBL; 9: 50 % PC/50 % GBL; 10: 70 % PC/30 % GBL; 11: 90 % PC/10 % GBL; 12: PC; 13: NMP.)

The influence of the donor number of solvent on the V_{oc} is related to the following three factors:

(1) The electron donor–acceptor reaction between organic solvent and triiodide [19]:

solvents + I_3^- → solvent … I_3^- ↔ solvents … I_2 + I^-

The above reaction equilibrium depends on the donor number of signal solvent or mixed solvent, the higher donor number of solvent leads to the incline of reaction equilibrium to the right [24–27], which gives a lower concentration of triiodide and causes a decrease of dark reaction eq. 5 and an increase of V_{oc} according to eq. 7.

$$V_{oc} = [\frac{kT}{e}] \ln\{\frac{I_{inj}}{n_{cb} k_{et} [I_3^-]}\} \quad (7)$$

where k is the Boltzmann constant, T is absolute temperature, e is an electronic charge, I_{inj} is the flux of charge resulting from sensitized injection, n_{cb} is the concentration of electrons on the surface of TiO_2, k_{et} is the reaction rate constant of I_3^- dark reaction on TiO_2 (eq. 5), $[I_3^-]$ is the concentration of I_3^- in liquid electrolyte.

(2) According to Grätzel's hypothesis [27], the reaction between the bare Lewis acidic TiO_2 surface and the Lewis basic solvent blocks the surface active sites of TiO_2, electrode which is responsible for the dark reaction eq. 5. The solvent with higher donor number has higher Lewis basicity, which shows a stronger function for blocking the active sites of TiO_2 electrode and decreasing the rate constant (k_{et}) of triiodide reduction. According to eq. 7, V_{oc} increases with the decreasing of k_{et}.

(3) The flatband potential (V_{fb}) of the TiO_2 electrode soaked in solvent was an important factor affecting V_{oc} [28], and the V_{fb} of TiO_2 electrode is sensitive to the contact solvent [1]. The contact solvent with higher donor number causes an increase in V_{fb} of the TiO_2 electrode [29]. Under Fermi lever pinning, these two parameters are linked by the following equation:

$$V_{oc} = | V_{fb} - V_{red} | \quad (8)$$

where V_{red} is the standard reduction potential of a redox couple, it remains constant [30]. So the V_{oc} increases with the increase of the donor number of solvent.

The decrease of J_{sc} is also related to the increasing of V_{fb} of TiO_2 electrode. The increase of V_{fb} also causes a negative shift in the conduction band edge of TiO_2, which decreases the energy bandgap between the conduction band of TiO_2 and photoexcited dye, and causes a decrease of driving force for the excited dye to inject electron into the conduction band of TiO_2. So the J_{sc} decreases with the increase of the donor number of solvent.

Redox couples

Although iodide/triiodide has been demonstrated as the most efficient redox couple for regeneration of the oxidized dye, its severe corrosion for many sealing materials, especially metals, causes a difficult assembling and sealing for a large-area DSSC and poor long-term stability of DSSC [31]. Therefore, other kinds of redox couples such as Br^-/Br_2, SCN^-/SCN_2, $SeCN^-/SeCN_2$ bipyridine cobalt (III/II) complexes were investigated for use in DSSCs, owing to their energy unmatchable with sensitized dyes or their intrinsic low diffusion coefficients in electrolyte, these redox couples show lower DSSCs' light-to-electricity conversion efficiencies than the iodide/triiodide redox couple does [5,32–36].

Cations in liquid electrolytes seem to function in the light-to-electricity conversion process of DSSCs. As a band bending and a depletion layer, which usually exist in bulk, semiconductor materials contacted with liquid electrolyte-containing redox couples [1] are considered unlikely in nanocrystalline TiO_2 electrodes owing to the extremely small size of the particle [37–38]. In fact, cations,

particularly small cations such as protons (Li^+, etc.) play an important role in the photoelectric performance of DSSCs. This is due to the fact that diffusion of electrons in the conduction band of TiO_2 is considered as an ambipolar diffusion mechanism, namely, ion diffusion is strongly correlated with electron transport to ensure that electrical neutrality is obeyed throughout the TiO_2 network [39–43]. For example, the addition of LiI into liquid electrolyte can enhance the J_{sc} of DSSCs. The reason is that the small-radius Li^+ can deeply penetrate into the mesoporous dye-coated nanocrystalline TiO_2 film and form an ambipolar Li^+-e^- with the electrons in the conduction band of TiO_2, which increases the transport speed of electrons in nanocrystalline TiO_2 network and enhances the J_{sc} of DSSCs [11,44,45]. However, the negative influence of ambipolar Li^+ on DSSCs is its easy combination with triiodide, which leads to the decrease of V_{oc} of the DSSCs [11,46]. In order to overcome this negative influence, an imidazole cation with larger ionic radii is used in liquid electrolyte to form a Helmholtz layer on the surface of TiO_2 film and block the direct contact of triiodide with ambipolar Li^+-e^-, which has an efficient result for suppressing the reaction between ambipolar Li^+-e^- and triiodide and enhancing the V_{oc} of the DSSC [44,46].

Electric additives

Electric additive is another important component in liquid electrolytes for optimizing the photovoltaic performance of DSSCs. It is found [27] that the photovoltaic performance of DSSCs can be enhanced hugely by adding a small amount of electric additive. The influence of nitrogen-containing heterocyclic additives on the photovoltaic performance of DSSCs was investigated, and it was found [47–53] that some efficient electric additives such as 4-*tert*-butylpyridine, pyridine could enhance V_{oc} but decrease J_{sc} owing to the same aforementioned reasons about the donor number of solvent on the photovoltaic performance of DSSC. The difference is that the function of electric additive for optimizing the photovoltaic performance of DSSCs is more efficient than that of the donor number of solvent. On the other hand, it is only a small amount of electric additive added into the electrolyte, the superfluous electric additive will cause a poor photovoltaic performance of DSSCs. Similar results also were found in our research [22,54].

Ionic liquids

Room-temperature ionic liquid (RTIL) has good chemical and thermal stability, negligible vapor pressure, nonflammability, and high ionic conductivity [55,56]. When incorporated into DSSCs, RTIL can be both the source of iodide and the solvent itself [57]. N. Papageorgiou et al. [58] reported in 1996 that these unique properties of RTIL were effective for long-term operation of electrochemical devices such as DSSCs. They employed methyl-hexyl-imidazolium iodide (MHImI) as an involatile electrolyte. The DSSC performance showed outstanding stability, with an estimated sensitizer redox turnover number in excess of 50 million. However, pure IL usually has higher viscosity than that of organic solvent, which limits the iodide/triioide transport speed and the restoration of oxidized dye, so the photovoltaic performance of these DSSCs is not so good as that of DSSCs using liquid electrolyte-containing organic solvents. In 2004, a solvent-free IL electrolyte-based $SeCN^-/(SeCN)_3^-$ redox couple was reported [59]. The viscosity of this IL, 1-ethyl-3-methylimidazolium selenocyanate (EMISeCN), was determined to be 25 cP at 21 °C, and the specific conductivity of EMISeCN was 14.1 mS/cm. Thus, an unprecedented 7.5–8.3 % light-to-electricity conversion efficiency under AM 1.5 sunlight was achieved for DSSCs. The low viscosity, higher conductivity, and visible-light absorbency of this kind of IL electrolyte ensure the high photovoltaic performance of DSSCs.

Liquid electrolyte-based organic solvent usually has high ionic conductivity and excellent interfacial contact property, which are the prerequisites for high photovoltaic performance of DSSCs. Although a photoelectric conversion efficiency of 11 % for the DSSC-containing liquid electrolyte has

been achieved [3–4], the potential problems caused by liquid electrolytes, such as leakage and volatilization of organic solvents, are considered as some of the critical factors limiting the long-term performance and practical use of DSSCs. Although the electrolyte using low-viscosity IL achieves a high photovoltaic performance for DSSCs, the sealing and leaking problems by liquid the same as liquid electrolytes with organic solvents still exist for high long-term stability of DSSCs. Thus, solid-state and quasi-solid-state electrolytes [6,8,21,60,62] with high long-term stability are attempted to replace liquid electrolytes.

SOLID-STATE ELECTROLYTES

Structure and operational principle of solid-state DSSCs

There are two kinds of solid-state DSSCs, one uses hole transport materials (HTMs) as medium, the other uses a solid-state electrolyte containing iodide/triiodide redox couple as medium. The structure and operational principle for the latter is similar to that of the DSSC using a liquid-state electrolyte containing iodide/triiodide redox couple as medium in Fig. 1. A schematic presentation [1,7] of the structure of solid-state DSSC using an HTM as medium is given in Fig. 4. At the heart of the system is a mesoporous TiO_2 film, which is placed in contact with a solid-state hole conductor. Attached to the surface of the nanocrystalline TiO_2 film is a monolayer of a charge-transfer dye. Photoexcitation of the dye results in the injection of an electron into the conduction band of the TiO_2. The original state of the dye is subsequently restored by electron donation from the hole conductor. The hole conductor is regenerated in turn at the counterelectrode, and the circuit is completed via electron migration through the external load [1,4]. In this DSSC, the reactions of excitation eq. 1, injection eq. 2, and recombination dark reaction eq. 6 still exist, the reaction eqs. 3–5 would be different [10].

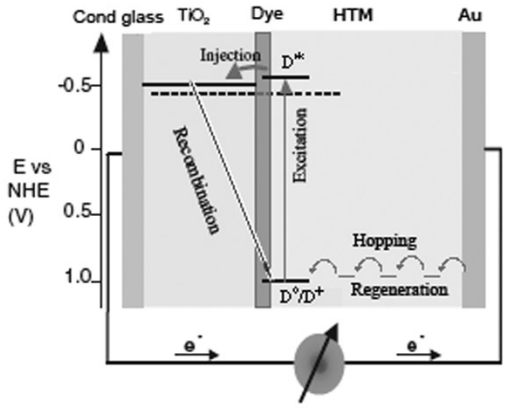

Fig. 4 Schematic diagram of charge transporting in solid-state DSSCs with HTMs.

Hole transport materials (HTMs)

Familiar large-bandgap HTMs such as SiC and GaN are not suitably used in DSSCs since the high-temperature deposition process for these materials will certainly degrade the sensitized dyes on the surface of nanocrystalline TiO_2 [10]. Researchers found [63–66] that a kind of inorganic HTM based on copper compounds such as CuI, CuBr, or CuSCN could be used in fabricating DSSCs. These copper-based materials can be cast from solution or vacuum deposition to form a complete hole-transporting layer, and CuI and CuSCN share good conductivity in excess of 10^{-2} S/cm, which facilitates their hole-conducting ability. For example [67], the DSSC based on CuI HTM obtained as high as 2.4 % light-to-electricity conversion efficiency under irradiation of AM 1.5, 100 mW·cm^{-2}. However, its stability is quite

poor, even worse than the traditional organic photovoltaic cell, which is also a common problem existing in DSSCs based on this kind of inorganic HTMs. Therefore, researchers put their vision into organic HTMs.

Organic HTMs have already been widely used in organic solar cells [71–74], organic thin film transistors [75–77], and organic light-emitting diodes [78–80]. Compared with inorganic HTMs, organic HTMs possess the advantages of plentiful sources, easy preparation, and low cost. In 1998, an efficient solid-state DSSC based on organic HTM 2,2',7,7'-tetrakis(*N*,*N*-di-*p*-methoxyphenylamine)9,9'-spirobifluorene (OMeTAD, Fig. 5) was reported [7], although the overall light-to-electricity conversion efficiency of this DSSC only reached 0.74 % under irradiation of 9.4 $mW \cdot cm^{-2}$, it is a pioneer for fabricating DSSCs with organic HTMs. Later, by improving the dye adsorption in the presence of silver ions in the dye solution [20,21], the efficiency of the solid-state DSSC employing spiro-OMeTAD was enhanced to 3.2 %, which is the highest level of the solid-state DSSCs by utilizing an organic transport material up to now. Table 1 lists the photovoltaic performance of DSSCs based on typical inorganic or organic HTMs, it can be seen that the overall light-to-electricity conversion efficiencies of these DSSCs are all much lower than that of the DSSCs based on liquid electrolytes. This is due to the low intrinsic conductivities of HTMs, the high frequencies of charge recombination from TiO_2 to HTMs, and the poor electronic contact between dye molecules and HTMs caused by incomplete penetration of solid HTMs into the pores of the mesoporous TiO_2 electrodes.

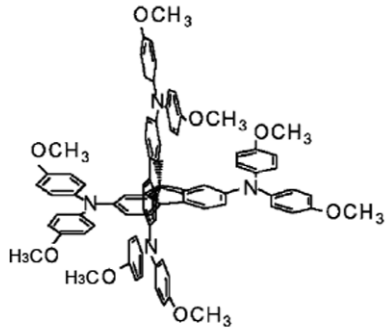

Fig. 5 Chemical structure of OMeTAD.

Table 1 Performance of solid-state DSSCs utilizing different HTMs.

HTM	Light-to-electricity conversion efficiency (%) (AM 1.5 100 $mW \cdot cm^{-2}$)	Reference
Inorganic HTM		
CuI	2.40	[67]
CuI	3.80	[68]
CuSCN	1.50	[65]
$4CuBr_3S(C_4H_9)_2$	0.60	[66]
Organic HTM		
OMeTAD	0.74* Irradiation with 9.4 $mW \cdot cm^{-2}$	[7]
OMeTAD	2.56	[20]
Spiro-OMeTAD	3.20	[21]
Pentacene	0.80	[69]
Polyaniline	1.15	[70]

Solid-state electrolyte-containing redox couple

Organic or inorganic HTM as a transport material for DSSCs cannot satisfy the practical application due to their low power conversion efficiencies. On the other hand, some remarkable results have already been achieved by introducing iodide/triioide redox couple into solid-state electrolytes as a transport medium for DSSCs. For example, a solid-state electrolyte containing iodide/triiodide redox couple by introducing TiO_2 nanoparticle into poly(ethylene oxide) (PEO) was prepared, the overall light-to-electricity conversion efficiency of 4.2 % for the DSSC with this solid-state electrolyte was obtained under irradiation of AM 1.5 100 mW·cm^{-2} [81]. A kind of ambient-temperature plastic crystal electrolyte containing iodide/triiodide redox couple was used to fabricate DSSCs and achieved a high overall light-to-electricity conversion efficiency of 6.5 % under irradiation of AM 1.5 100 mW·cm^{-2} [82]. A solid-state electrolyte based on $LiIC_6H_{10}N_2O_2$ [$LiI(HPN)_2$] single crystal (shown in Fig. 6) and iodide/triiodide was prepared. This solid-state electrolyte can be optimized by adding SiO_2 nanoparticles and put into DSSCs to enhance light-to-electricity conversion efficiency without adding iodide molecules [83]. Higher photovoltaic performance for DSSCs using iodide/triiodide redox couple than that using HTMs is due to the fact that the iodide/triiodide can efficiently revivify oxidized dyes, and the dark reactions in these solid-state electrolytes are lower than that in HTMs. Another reason is that the interfacial contact properties of these solid-state electrolytes are better than that of HTMs. This kind of solid-state electrolyte has a good prospect in practical DSSCs.

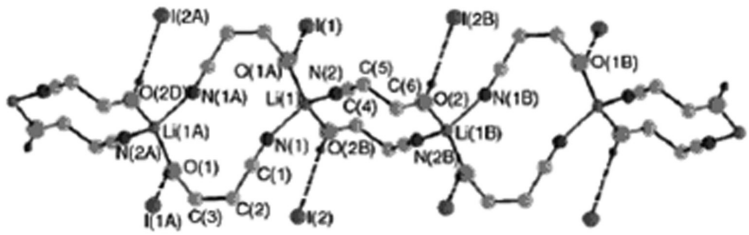

Fig. 6 Structure of $LiI(HPN)_2$.

QUASI-SOLID-STATE ELECTROLYTES

The quasi-solid state, or gel state, is a particular state of matter, neither liquid nor solid, or conversely both liquid and solid. Generally, a quasi-solid-state electrolyte is defined as a system which consists of a polymer network (polymer host) swollen with liquid electrolytes [6,84–88]. Owing to its unique hybrid network structure, quasi-solid-state electrolytes always possess, simultaneously, both the cohesive property of a solid and the diffusive transport property of a liquid. Namely, quasi-solid-state electrolytes show better long-term stability than liquid electrolytes do and have the merits of liquid electrolytes including high ionic conductivity and excellent interfacial contact property [5,84,85]. These unique characteristics of quasi-solid-state electrolytes have been actively developed as highly conductive electrolyte materials for DSSCs, lithium secondary batteries, and fuel cells [86]. Quasi-solid-state electrolytes are usually prepared by incorporating a large amount of a liquid electrolyte into organic monomer or polymer matrix, forming a stable gel with a network structure via a physical or chemical method. The quasi-solid-state electrolyte formed via physical cross-linking is called "entanglement network", which is thermo-reversible (thermoplastic). By contrast, chemical or covalent cross-linking leads to the formation of thermo-irreversible (thermosetting) gel electrolyte [5].

Thermoplastic gel electrolytes (TPGEs)

The formation of the TPGE is based on physical cross-linking of gelators to form a "entanglement network" to solidify liquid electrolyte. The main characteristic of this kind of gel electrolyte is the gel-sol state reversible conversion with the change of temperature, which is a benefit of deep penetration of the electrolyte into mesoporous dye-coated nanocrystalline TiO_2 film [5,10,87]. The interfacial contact between the electrolyte layer and nanocrystalline TiO_2 film or counterelectrode is one of the most important factors influencing the photovoltaic performance of DSSCs besides the ionic conductivity of the gel electrolyte [60].

The TPGE contains gelator and liquid electrolyte, the liquid electrolyte consists of organic solvent, redox couple, additive, or IL electrolyte system. The first thermoplastic polymer gel electrolyte used in DSSCs was reported [89]. The electrolyte was composed of poly(acrylonitrile) (PAcN), EC, PC, AcN, and NaI. The light-to-electricity conversion efficiency of this DSSC was lower in comparison with that of the DSSC based on liquid electrolytes, due to the unoptimized components and the difficult penetration of the PAcN network into nanocrystalline TiO_2 film [90,91]. The high photovoltaic performance and excellent stability of DSSC was obtained by using a TPGE containing poly(vinylidene-fluoride-*co*-hexafluoropropylene) (PVDF–HFP) combined with MePN-based liquid electrolyte containing 1,2-dimethyl-3-propyl imidazolium iodide and iodide [6]. The DSSC showed a similar photovoltaic performance as that of an analogous cell containing the same liquid electrolyte, which means that the polymer matrix has no negative effect on the performance of DSSC.

A TPGE based on 1,3:2,4-di-*O*-dimethylbenzylidene-D-sorbitol/MePN (Fig. 7) was prepared [87], and a stable overall light-to-electricity conversion efficiency of 6.1 % for the DSSC using the TPGE was achieved under AM 1.5 sunlight illumination (99.8 $mW \cdot cm^{-2}$). On the other hand [92], a gel electrolyte with a low-molecular-weight gelator (Fig. 8), an IL, 1-alkyl-3-methylimidazolium iodide, and iodide was prepared, the DSSC based on the gel electrolyte showed a 5.0 % light-to-electricity conversion efficiency under irradiation of AM 1.5 100 $mW \cdot cm^{-2}$.

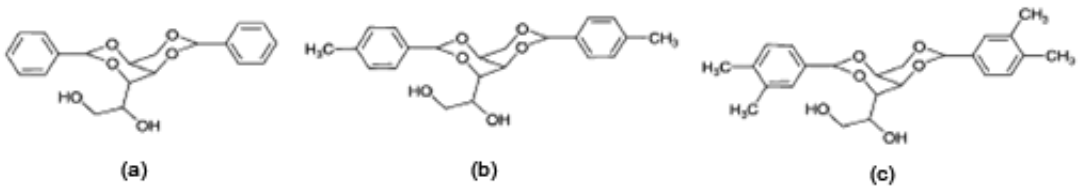

Fig. 7 Chemical structures of sorbitol derivatives (a) 1,3:2,4-di-*O*-benzylidene-D-sorbitol; (b) 1,3:2,4-di-*O*-methyl-benzylidene-D-sorbitol; (c) 1,3:2,4-di-*O*-dimethyl-benzylidene-D-sorbitol.

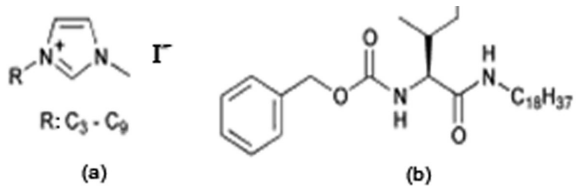

Fig. 8 Chemical structures of (a) 1-alkyl-3-methylimidazolium iodides and (b) gelator.

Recently, our research group have been focusing on the thermoplastic and thermosetting gel electrolytes for DSSCs [8,22,62,93–100], we reported a novel TPGE [8] using poly(ethylene glycol) (PEG) as polymer host, PC as solvent, potassium iodide, and iodide as ionic conductor. Based on the TPGE, a stable DSSC with an overall light-to-electricity conversion efficiency of 7.22 % was achieved. The TPGE exhibits a thermoplastic character, high conductivity, and long-term stability, and can be prepared by a simple and convenient protocol. The viscosity, conductivity, and phase state of the TPGE can be controlled by tuning the composition. The present findings should accelerate the widespread use of DSSCs. There are some important characteristics for the TPGE:

(1) PEG contains many ether groups and polyhydric side groups, two kind of groups can keep complexation with alkali metal ions such as potassium ions, sodium ions [101]. Because of the interaction between PEG and PC and alkali metal iodide salts, the iodide anions can be separated from alkali cations to form free anions as shown in Fig. 9a.

(2) The large amount of ether groups and polyhydric side groups on the PEG matrix can form a hydrogen bond with PC solvent, which hangs the molecule of solvent on the "entanglement network" of the polymer chain, and results in the formation of a stable thermo-reversible polymer gel electrolyte as shown in Fig. 9b.

(3) The TPGE is in a solid state and shows the fluidity (Fig. 10) with a viscosity of 0.76 Pa s at a temperature higher than 50 °C, which makes for a deep penetration into the mesoporous dye-coated nanocrystalline TiO_2 film [102], and forms a sufficient interfacial contact between electrolyte layer and nanocrystalline TiO_2 film and platinum counterelectrode. Whereas at a temperature below 20 °C, the TPGE is in a gel state with a viscosity of 2.17 Pa s. The reversible thermoplastic behavior of the TPGE is very useful for sealing and assembling DSSCs.

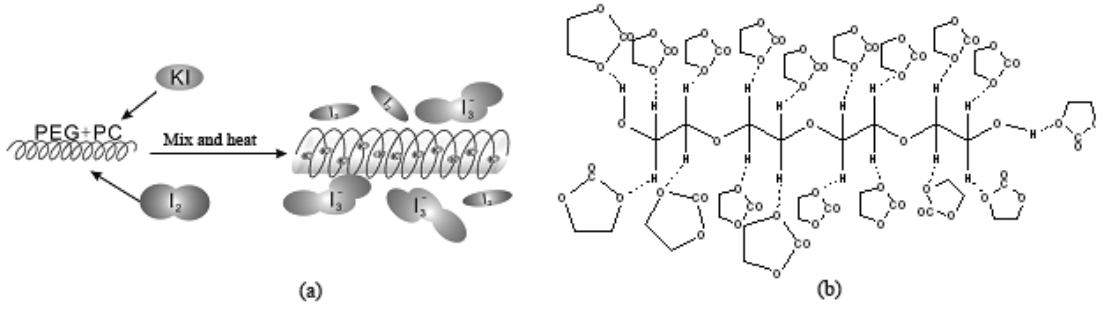

Fig. 9 Interaction between PEG polymer matrix, PC solvent, and KI salts (a) and its chemical structure (b).

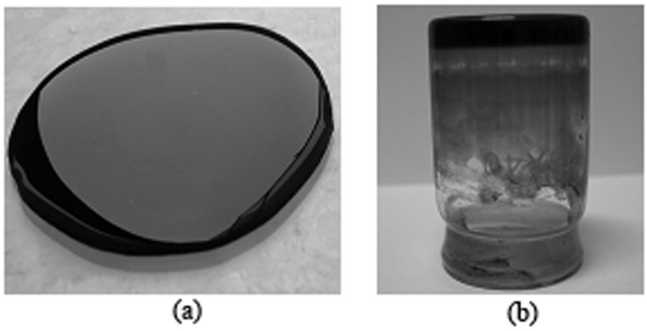

Fig. 10 TPGE based on PEG/PC/KI+I_2 system at 50 °C (a) and at 15 °C (b).

The characteristics of the thermoplastic polymer gel electrolyte markedly depends on temperature. This is due to the fact that the increase of temperature causes a phase transfer from gel state to sol state, and a change of dominate conduction mechanism from Arrhenius type to Vogel–Tamman–Fulcher (VTF) type as shown in Fig. 11, which turns to the change of ionic conductivity of thermoplastic polymer gel electrolyte and photovoltaic performance of DSSC. It can be seen from Fig. 12 that the photovoltaic performance of DSSCs severely depends on the temperature, which is the typical characteristic of DSSCs based on this kind of polymer gel electrolyte.

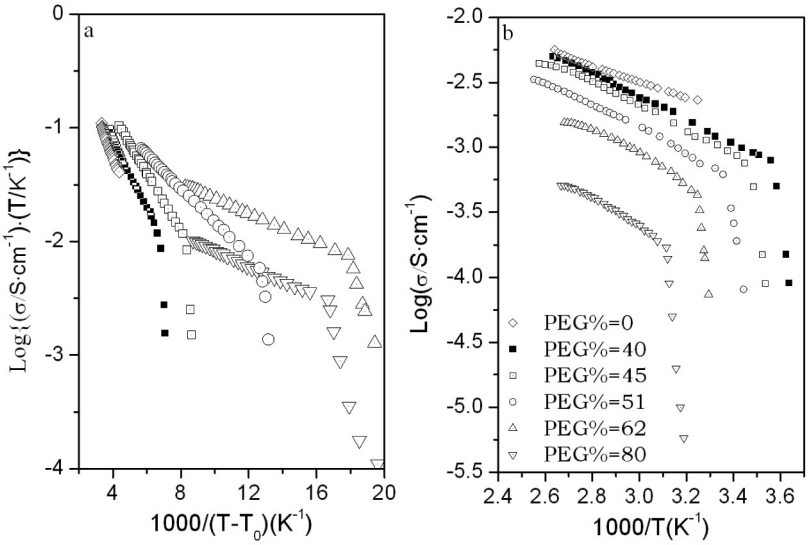

Fig. 11 Temperature vs. the conductivity of TPGE with different PEG concentrations. (a) VTF plots, (b) Arrhenius plots. The concentration of I^- and I_2 is 0.1 and 0.01 M, respectively.

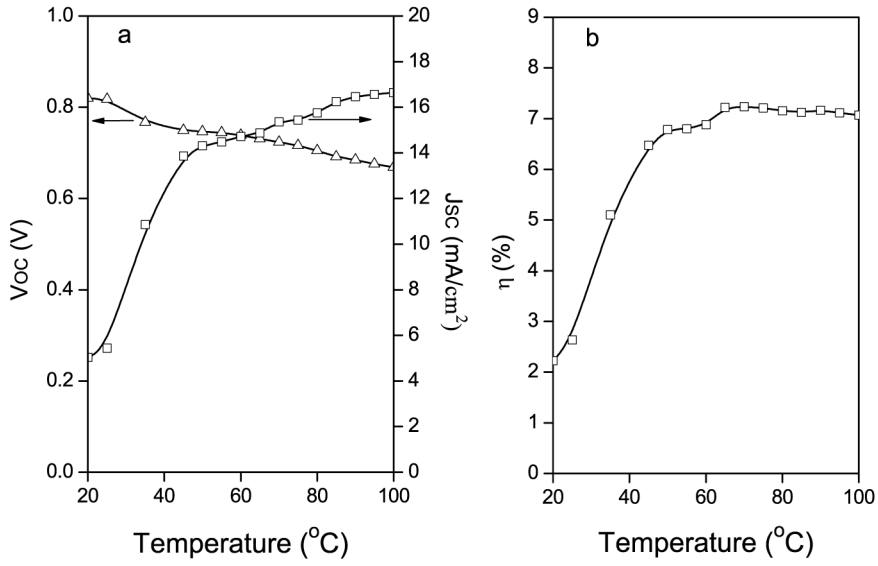

Fig. 12 Effect of temperature on the performance of quasi-solid-state DSSC with TPGE based on PEG/PC/KI+I_2 system. The irradiation intensity is 100 mW·cm^{-2}.

Thermosetting gel electrolytes (TSGEs)

The TPGE is good for fabricating DSSCs. However, there is also a potential venture for actual application of DSSCs, which is the chemical unstability, such as phase-separation, crystallization of iodide salts. Therefore, some more environmentally stable electrolytes are still needed. Among those optional methods, the TSGE is one of the good selections for high photovoltaic performance and good long-term stability of DSSCs.

A high stable DSSC based on a TSGE containing ureasil precursors (Fig. 13) and organic liquid electrolyte containing iodide salts was prepared [60,103–105]. The unique structure of this thermosetting organic–inorganic hybrid gel electrolyte leads to the high quality of DSSC, which maintains 5–6 % light-to-electricity conversion efficiency even after preserving for several years.

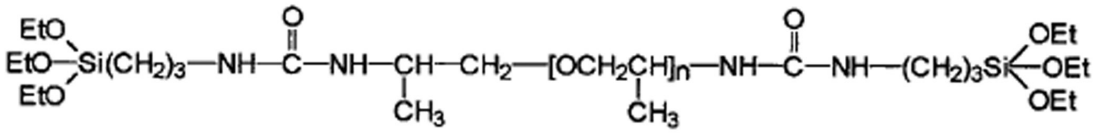

Fig. 13 Ureasil precursor structures.

Recently, we reported a novel TSGE based on poly(acrylic acid)-poly(ethylene glycol) (PAA–PEG) hybrid and liquid electrolyte for fabricating a high-performance and stable DSSC [9,62,97,98]. It is known that PAA polymer matrix shows excellent hydrogel stability due to the formation of 3D networks structure in hydrogel and the strong interaction between absorbed aqueous solution and hydrophilic groups in PAA [106,107]. PAA is a kind of oleophobic polymer, which cannot dissolve or swell in organic solvents. By modifying PAA with amphiphilic PEG, the PAA–PEG hybrid shows a moderate liquid electrolyte absorbency in some organic Lewis basic liquid electrolytes. The optimized Lewis basic organic mixed solvents for both PAA–PEG hybrid and photovoltaic performance of DSSC was obtained by mixing 30 vol % NMP with 70 vol % GBL [22]. The TSGE with ionic con-

ductivity of 6.12 mS cm^{-1} was obtained by swelling the PAA–PEG hybrid in the optimized Lewis basic organic mixed solvents containing iodide/triiodide redox couple (Fig. 14). Based on the TSGE, a DSSC with light-to-electricity conversion efficiency of 6.10 % was attained under AM 1.5 irradiation.

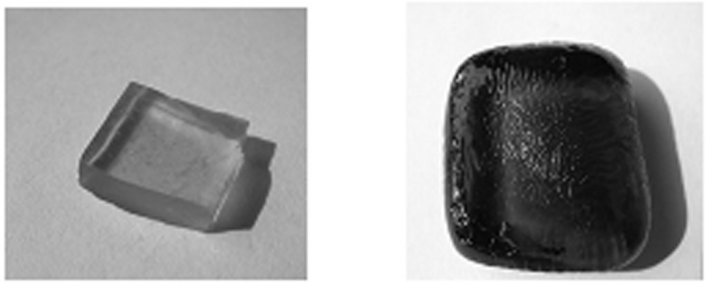

Fig. 14 TSGE based on PAA–PEG system before (a) and after (b) soaking in liquid electrolyte.

The dominate conduction mechanism of this kind of TSGE mainly depends on the amount of absorbed liquid electrolyte. As shown in Fig. 15, excepting the TSGE based on PAA–PEG 400, the lnσ vs. 1/T plots of other TSGEs and liquid electrolytes conform to the Arrhenius type. The lower liquid electrolyte absorbency of TSGE based on PAA–PEG 400 (shown in Fig. 16) leads to the dominate influence of polymer matrix in ion transport and the departure of its lnσ vs. 1/T plots from Arrhenius-type straight line. The DSSC based on this TSGE shows a high photovoltaic performance and an excellent stability as shown in Table 2 and Fig. 17.

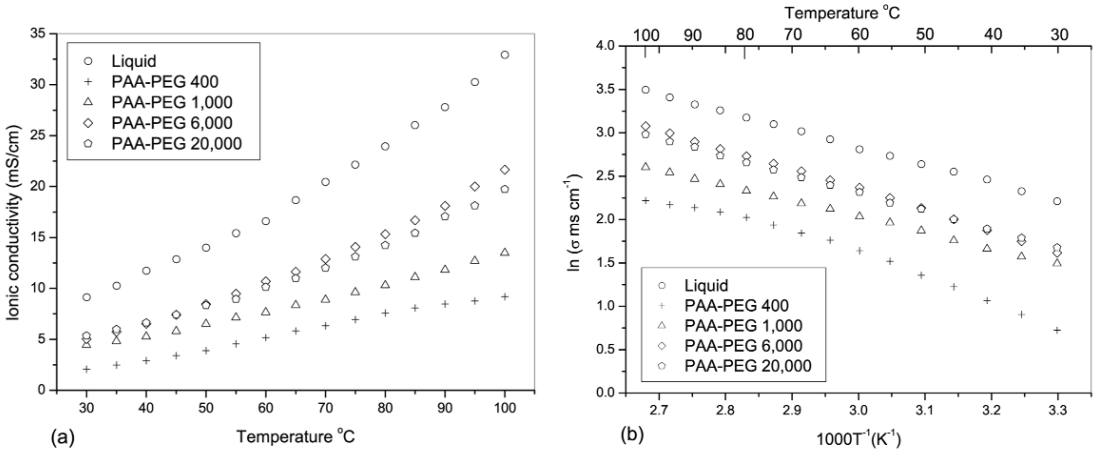

Fig. 15 Temperature vs. ionic conductivity of the TSGE based on PAA–PEG hybrid (a) and its Arrhenius plots (b).

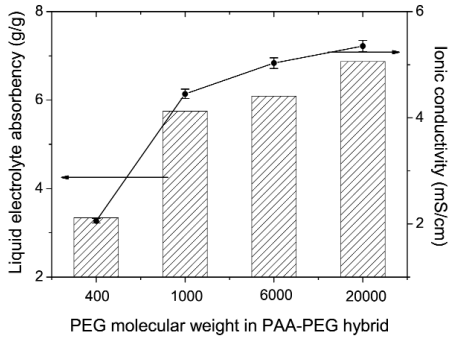

Fig. 16 Liquid absorbency and ionic conductivity of the TSGE based on PAA–PEG vs. PEG molecular weight.

Table 2 Photovoltaic performance of DSSCs with different electrolytes.

Electrolyte	σ (mS·cm^{-1})	V_{oc} (V)	J_{sc} (mA·cm^{-2})	*FF*	*Eff* (%)
Liquid **a**	9.13	0.632	14.78	0.613	5.73
Liquid **b**	8.64	0.705	13.34	0.712	6.70
TSGE	6.12	0.735	12.55	0.661	6.10

Liquid **a**: containing 0.5 M NaI, 0.05 M I_2 in 30 vol % NMP, and 70 vol % GBL mixed solvents.
Liquid **b**: adding 0.4 M pyridine into liquid **a**.
TSGE: thermosetting gel electrolyte prepared by soaking PAA–PEG hybrid in liquid **b**.

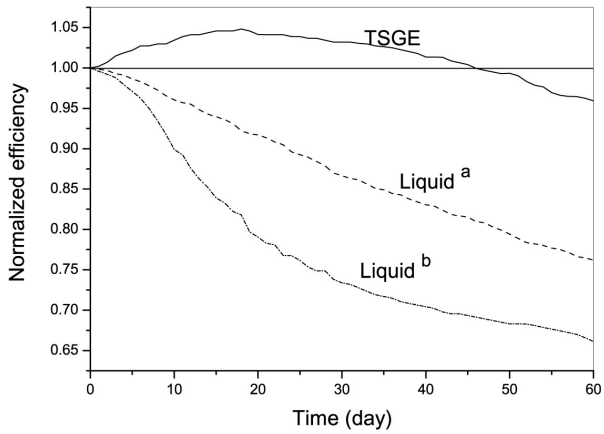

Fig. 17 Long-term stabilities of DSSCs with liquid electrolyte **a**, liquid electrolyte **b**, and the TSGE based on PAA–PEG.

CONCLUSIONS

In this review, we introduce the recent progress, including our group results, on liquid, solid-state, and quasi-solid-state electrolytes for DSSCs. Although a light-to-electricity conversion efficiency of 11 % for DSSCs containing liquid electrolytes has been achieved, the potential problems caused by liquid electrolytes, such as leakage and volatilization of organic solvents, are considered as some of the critical factors limiting the long-term performance and practical use of DSSCs. Solid-state electrolytes overcome the disadvantage of fluidity and volatility for liquid electrolytes, however, poor interface contact

property and lower conductivity for solid-state electrolytes lead to lower light-to-electricity conversion efficiency for DSSCs. Quasi-solid-state electrolytes, especially TSGEs, possess liquid electrolyte's ionic conductivity and interface contact property and solid-state electrolyte's long-term stability, it is believed to be one kind of the most available electrolytes for fabricating high photoelectric performance and long-term stability of DSSCs in practical applications.

ACKNOWLEDGMENTS

The authors gratefully acknowledge the financial support of the National Natural Science Foundation of China (Nos. 50572030, 50372022), the Nano Functional Materials Special Program of Fujian Province, China (No. 2005HZ01-4), the Key Science and Technology Program by the Ministry of Education, China (No. 206074), and Specialized Research Fund for the Doctoral Program of Chinese Higher Education (No. 20060385001).

REFERENCES

1. M. Grätzel. *Nature* **414**, 338 (2001).
2. B. O'Regan, M. Grätzel. *Nature* **353**, 737 (1991).
3. M. Grätzel. *Inorg. Chem.* **44**, 6841 (2005).
4. M. Grätzel. *J. Photochem. Photobiol., A* **164**, 3 (2004).
5. A. F. Nogueira, C. Longo, M. A. De Paoli. *Coord. Chem. Rev.* **248**, 1455 (2004).
6. P. Wang, S. M. Zakeeruddin, J. E. Moser, T. Sekiguchi, M. Grätzel. *Nat. Mater.* **2**, 402 (2003).
7. U. Bach, D. Lupo, P. Comte, J. E. Moser, F. Weissortel, J. Salbeck, H. Spreitzer, M. Grätzel. *Nature* **395**, 583 (1998).
8. J. H. Wu, S. C. Hao, Z. Lan, J. M. Lin, M. L. Huang, Y. F. Huang. *Adv. Funct. Mater*. **17**, 2645 (2007).
9. J. H. Wu, Z. Lan, J. M. Lin, M. L. Huang, S. C. Hao, T. Sato, S. Yin. *Adv. Mater*. **19**, 4006 (2007).
10. B. Li, L. D. Wang, B. Kang, P. Wang, Y. Qiu. *Sol. Energy Mater. Sol. Cells* **90**, 549 (2006).
11. A. J. Frank, N. Kopidakis, J. V. D. Lagemaat. *Coord. Chem. Rev.* **248**, 1165 (2004).
12. S. A. Haque, E. Palomares, B. M. Cho, A. N. M. Green. *J. Am. Chem. Soc.* **127**, 3456 (2005).
13. A. Hagfeldt, M. Grätzel. *Chem. Re*v. **95**, 49 (1995).
14. N. S. Sariciftci, L. Smilowitz, A. J. Heeger, F. Wudl. *Science* **258**, 1474 (1992).
15. G. Benko, J. Kallioinen, A. P. Yartsev, V. Sundstrom. *J. Am. Chem. Soc*. **124**, 489 (2002).
16. J. Schnadt, P. A. Bruhwiler, L. Patthey, J. N. O'Shea, S. Sodergren. *Nature* **418**, 620 (2002).
17. W. Stier, W. R. Duncan, O. V. Prezhdo. *Adv. Mater*. **16**, 240 (2004).
18. J. Ashbury, E. Hao, Y. Wang, H. N. Ghosh, T. Lian. *J. Phys. Chem. B* **105**, 4545 (2001).
19. Z. Kebede, S. E. Lindquist. *Sol. Energy Mater. Sol. Cells* **57**, 259 (1999).
20. A. Fukui, R. Komiya, R. Yamanaka, A. Islam. *Sol. Energy Mater. Sol. Cells* **90**, 649 (2006).
21. S. C. Hao, J. H. Wu, L. Q. Fan, Y. F. Huang, J. M. Lin, Y. L. Wei. *Sol. Energy* **76**, 745 (2004).
22. J. H. Wu, Z. Lan, J. M. Lin, M. L. Huang. *J. Power Sources* **173**, 585 (2007).
23. K. Haraa, T. Horiguchib, T. Kinoshitab, K. Sayamaa. *Sol. Energy Mater. Sol. Cells* **70**, 151 (2001).
24. D. Cahen, G. Hodes, M. Grätzel, J. F. Guillemoles, I. Riess. *J. Phys. Chem. B* **104**, 2053 (2000).
25. S. Y. Huang, G. Schlichthorl, A. M. Grätzel, A. J. Frank. *J. Phys. Chem. B* **101**, 2576 (1997).
26. G. Schlichthorl, S. Y. Huang, J. Sprague, A. J. Frank. *J. Phys. Chem. B* **101**, 8141 (1997).
27. M. K. Nazeetuddin, M. Grätzel. *J. Am. Chem. Soc.* **115**, 6382 (1993).
28. T. S. Kang, K. H. Chun, J. S. Hong, S. H. Moon, K. J. Kim. *J. Electrochem. Soc.* **147**, 3049 (2000).
29. J. S. Hong, M. Joo, R. Vittal, K. J. Kim. *J. Electrochem. Soc. E* **149**, 493 (2002).
30. I. P. Alexander, D. H. Geske. *J. Am. Chem. Soc*. **80**, 1340 (1958).

31. M. Toivola, F. Ahlskog, P. Lund. *Sol. Energy Mater. Sol. Cells* **90**, 2881 (2006).
32. Z. S. Wang, K. Sayama, H. Sugihara. *J. Phys. Chem. B* **109**, 22449 (2005).
33. B. V. Bergeron, A. Marton, G. Oskam. *J. Phys. Chem. B* **109**, 937 (2005).
34. G. Oskam, B. V. Bergeron, G. J. Meyer. *J. Phys. Chem. B* **105**, 6867 (2001).
35. S. A. Sapp, C. M. Elliott, C. Contado. *J. Am. Chem. Soc.* **124**, 11215 (2002).
36. H. Nusbaumer, J. E. Moser, S. M. Zakeeruddin. *J. Phys. Chem. B* **105**, 10461 (2001).
37. M. Grätzel, A. J. Frank. *J. Phys. Chem.* **86**, 2964 (1982).
38. A. Hagfeldt, M. Grätzel. *Chem. Rev.* **95**, 49 (1995).
39. J. V. D. Lagemaat, N. G. Park, A. J. Frank. *J. Phys. Chem. B* **104**, 2044 (2000).
40. N. Kopidakis, E. A. Schiff, N. G. Park, A. J. Frank. *J. Phys. Chem. B* **104**, 3930 (2000).
41. A. Solbrand, H. Lindstrom, A. Hagfeldt, S. E. Lindquist. *J. Phys. Chem. B* **101**, 2514 (1997).
42. A. Zaban, A. Meier, B. Gregg. *J. Phys. Chem. B* **101**, 7985 (1997).
43. D. Nister, K. Keis, S. E. Lindquist, A. Hagfeldt. *Sol. Energy Mater. Sol. Cells* **73**, 411 (2002).
44. C. L. Olson. *J. Phys. Chem. B* **110**, 9619 (2006).
45. Y. Liu, A. Hagfeldt, X. R. Xiao, S. E. Lindquist. *Sol. Energy Mater. Sol. Cells* **55**, 267 (1998).
46. D. F. Watson, G. J. Meyer. *Coord. Chem. Rev.* **248**, 1391 (2004).
47. H. Kusama, H. Arakawa. *Sol. Energy Mater. Sol. Cells* **81**, 87 (2004).
48. H. Kusama, H. Arakawa. *Sol. Energy Mater. Sol. Cells* **82**, 457 (2004).
49. H. Kusama, H. Arakawa. *J. Photochem. Photobiol., A* **164**, 103 (2004).
50. H. Kusama, H. Arakawa. *J. Photochem. Photobiol., A* 1**62**, 441 (2004).
51. H. Kusama, M. Kurashige, H. Arakawa. *J. Photochem. Photobiol., A* **169**, 169 (2005).
52. H. Kusama, H. Arakawa. *Sol. Energy Mater. Sol. Cells* **85**, 333 (2005).
53. H. Kusama, H. Arakawa. *J. Photochem. Photobiol., A* **165**, 157 (2004).
54. Z. Lan, J. Wu, J. Lin, M. Huang, P. Li, Q. Li. *Electrochim. Acta* **53**, 2296 (2008).
55. H. Matsumoto, T. Matsuda, T. Tsuda, R. Hagiwara, Y. Ito, Y. Miyazaki. *Chem. Lett.* 26 (2001).
56. P. Wang, S. M. Zakeeruddin, J. E. Moser, M. Grätzel. *J. Phys. Chem. B* **107** 13280 (2003).
57. T. Kitamura, M. Maitani, M. Matsuda, Y. Wada, S. Yanagida. *Chem. Lett.* 1054 (2001).
58. N. Papageorgiou, Y. Athanassov, M. Armand, P. Bonhote, H. Pettersson, A. Azam, M. Grätzel. *J. Electrochem. Soc.* **143**, 3099 (1996).
59. P. Wang, S. M. Zakeeruddin, J. E. Moser, R. H. Baker, M. Grätzel. *J. Am. Chem. Soc.* **126**, 7164 (2004).
60. E. Stathatos, P. Lianos, U. Lavrencic-Stangar, B. Orel. *Adv. Mater.* **14**, 354 (2002).
61. Y. J. Kim, J. H. Kim, M. S. Kang, M. J. Lee, J. Won, J. C. Lee, Y. S. Kang. *Adv. Mater.* **16**, 1753 (2004).
62. Z. Lan, J. H. Wu, J. M. Lin, M. L. Huang. *J. Power Sources* **164**, 921 (2007).
63. K. Tennakone, G. Kumara, A. R. Kumarasinghe, K. G. U. Wijayantha, P. M. Sirimanne. *Semicond. Sci. Technol.* **10**, 1689 (1995).
64. G. Kumara, A. Konno, G. K. R. Senadeera, P. V. V. Jayaweera, D. D. Silva, K. Tennakone. *Sol. Energy Mater. Sol. Cells* **69**, 195 (2001).
65. B. O'Regan, D. T. Schwartz. *Chem. Mater.* **10**, 1501 (1998).
66. K. Tennakone, G. K. R. Senadeera, D. D. Silva, I. R. M. Kottegoda. *Appl. Phys. Lett.* **77**, 2367 (2000).
67. K. Tennakone, V. P. S. Perera, I. R. M. Kottegoda, G. Kumara. *J. Phys. D* **32**, 374 (1999).
68. Q. B. Meng, K. Takahashi, X. T. Zhang, I. Sutanto, T. N. Rao, O. Sato, A. Fujishima, H. Watanabe, T. Nakamori, M. Uragami. *Langmuir* **19**, 3572 (2003).
69. G. K. R. Senadeera, P. V. V. Jayaweera, V. P. S. Perera, K. Tennakone. *Sol. Energy Mater. Sol. Cells* **73**, 103 (2002).
70. S. X. Tan, J. Zhai, M. X. Wan, Q. B. Meng, Y. L. Li, L. Jiang, D. B. Zhu. *J. Phys. Chem. B* **108**, 18693 (2004).
71. L. Sicot, C. Fiorini, A. Lorin, J. M. Nunzi, P. Raimond, C. Sentein. *Synth. Met.* **102**, 991 (1999).

72. M. Catellani, B. Boselli, S. Luzzati, C. Tripodi. *Thin Solid Films* **66**, 403 (2002).
73. J. H. Schon, C. Kloc, E. Bucher, B. Batiogg. *Nature* **403**, 408 (2000).
74. S. E. Shaheen, C. J. Brabec, N. S. Sariciftci, F. Padinger, T. Fromherz, J. C. Hummelen. *Appl. Phys. Lett.* **78**, 841 (2001).
75. H. Sirringhaus, P. J. Brown, R. H. Friend, M. M. Nielsen. *Nature* **401**, 685 (1999).
76. Y. Y. Lin, D. J. Gundlach, S. F. Nelson, T. N. Jackson. *IEEE Electron. Device Lett.* **18**, 606 (1997).
77. H. E. Katz, J. G. Laquindanum, A. J. Lovinger. *Chem. Mater.* **10**, 633 (1998).
78. C. W. Tang, S. A. VanSlyke. *Appl. Phys. Lett.* **51**, 913 (1987).
79. S. A. VanSlyke, C. H. Chen, C. W. Tang. *Appl. Phys. Lett.* **69**, 2160 (1996).
80. L. S. Hung, C. W. Tang, M. G. Mason. *Appl. Phys. Lett*. **70**, 152 (1997).
81. T. Stergiopoulos, L. M. Arabatzis, G. Katsaros. *Nano Lett.* **2**, 1259 (2002).
82. P. Wang, Q. Dai, S. M. Zakeeruddin. *J. Am. Chem. Soc*. **126**, 13590 (2004).
83. H. Wang, H. Li, Q. Meng. *J. Am. Chem. Soc*. **127**, 6394 (2005).
84. S. B. R. Murphy. In *Polymer Networks—Principles of Their Formation, Structure and Properties*, R. F. T. Stepto (Ed.), Blackie Academic, London (1998).
85. S. Megahed, B. Scrosati. *Interface* **4**, 34 (1995).
86. K. M. Abraham. In *Application of Electroactive Polymer*, B. Scrosati (Ed.), Chapman & Hall, London (1993).
87. N. Mohmeyer, P. Wang, H. W. Schmidt, S. M. Zakeeruddin, M. Grätzel. *J. Mater. Chem*. **14**, 1905 (2004).
88. J. Y. Song, Y. Y. Wang, C. C. Wan. *J. Power Sources* **77**, 183 (1999).
89. F. Cao, G. Oskam, P. C. Searson. *J. Phys. Chem. B* **99**, 17071 (1995).
90. Y. Reng, Z. Zhang, E. Gao, S. Fang, S. Cai. *J. Appl. Electrochem*. **31**, 445 (2001).
91. M. Matsumoto, H. Miyasaki, K. Matsuhiro, Y. Kumashiro, Y. Takaoka. *Solid State Ionic* **89**, 263 (1996).
92. W. Kubo, T. Kitamura, K. Hanabusa, Y. Wada, S. Yanagida. *Chem. Commun.* 374 (2002).
93. Z. Lan, J. H. Wu, D. B. Wang, S. C. Hao, J. M. Lin, Y. F. Huang. *Sol. Energy* **80**, 1483 (2006).
94. Z. Lan, J. H. Wu, D. B. Wang, S. C. Hao, J. M. Lin, Y. F. Huang. *Sol. Energy* **81**, 117 (2007).
95. J. H. Wu, Z. Lan, D. B. Wang, S. C. Hao, J. M. Lin. *J. Photochem. Photobiol., A* **181**, 333 (2006).
96. J. H. Wu, Z. Lan, D. B. Wang, S. C. Hao, J. M. Lin. *Electrochim. Acta* **51**, 4243 (2006).
97. Z. Lan, J. H. Wu, J. M. Lin, M. L. Huang, S. Yin, T. Sato. *Electrochim. Acta* **52**, 6673 (2007).
98. J. H. Wu, Z. Lan, J. M. Lin, M. L. Huang, S. C. Hao. *Electrochim. Acta* **52**, 7128 (2007).
98. J. H. Wu, P. J. Li, S. C. Hao, H. X. Yang, Z. Lan. *Electrochim. Acta* **52**, 5334 (2007).
99. M. L. Huang, H. X. Yang, J. H. Wu, J. M. Lin, Z. Lan, P. J. Li, S. C. Hao. *J. Sol-Gel. Sci. Technol.* **42**, 65 (2007).
100. J. H. Wu, S. C. Hao, J. M. Lin, M. L. Huang, Y. F. Huang, Z. Lan, P. J. Li. *Cryst. Growth Des.* **8**, 247 (2008).
101. J. H. Kim, M. S. Kang, Y. J. Kim, J. Won, Y. S. Kang. *Solid State Ionics* **176**, 579 (2005).
102. M. S. Kang, J. H. Kim, J. Won, Y. S. Kang. *J. Photochem. Photobiol., A* **183**, 15 (2006).
103. E. Stathtos, P. Lianos, C. Krontiras. *J. Phys. Chem. B* **105**, 3486 (2001).
104. E. Stathtos, P. Lianos, U. L. Stangar, B. Orel. *Adv. Funct. Mater*. **14**, 45 (2004).
105. E. Stathtos, P. Lianos. *Chem. Mater.* **15**, 1825 (2003).
106. J. H. Wu, J. M. Lin, M. Zhou. *Macromol. Rapid Commun.* **21**, 1032 (2000).
107. J. M. Lin, J. H. Wu, Z. F. Yang, M. L. Pu. *Macromol. Rapid Commun.* **22**, 422 (2001).